16th World Congress in Computational Mechanics (WCCM)
21-26 July 2024, Vancouver, Canada
A. Korobenko, M. Laforest, S. Prudhomme, R. Vaziri (Eds)

HYPER-DIMENSIONAL GAP FINITE ELEMENTS FOR THE ENFORCEMENT OF INTERFACIAL CONSTRAINTS

Brian D. Giffin[1]

[1] Oklahoma State University
228 Engineering North, Stillwater, OK 74078-5013
brian.giffin@okstate.edu; https://experts.okstate.edu/brian.giffin

Key words: Contact Problems, Domain Interface Method, Mortar Method, FEM.

Abstract. In the classical theory of two-body contact, a single shared contact interface is considered between two continuum bodies, and is further discretized as such in the finite element setting. In general, however, the finite element mesh topology of two contacting bodies will be non-conforming at this shared interface, requiring the definition of a preferred or intermediate surface over which integral constraints may be evaluated. The specification of this interface is deemed to be somewhat arbitrary, but in practice the numerical solution of contact problems may exhibit sensitivity to the particular choice of intermediate surface. A further complication concerns the need to establish projective mappings between the discretized finite element surfaces and the chosen intermediate surface, particularly for the sake of evaluating the contact gap function between pairs of points on each of the two bodies.

In this work, a new methodology for the enforcement of contact constraints in the context of finite element analyses is proposed. The method entails an alternative representation of contact surface integrals by equivalently integrating over the interstitial – albeit degenerate gap volume between two contacting bodies. An auxiliary indicator field is defined on each body, and is used to represent the degenerate interstitial volume as a non-degenerate hyper-dimensional gap volume. Over this domain, the gradient of the continuously interpolated displacement field with respect to the indicator field yields the oriented displacement gap, which may be used in the formulation of contact inequality constraints. Discretization of the hyper-dimensional gap volume into conforming finite elements is explored, and is observed to offer several advantages over existing contact discretization methods: the proposed method does not require the computation of geometric intersections or projections; it exploits conventional Gaussian quadrature schemes to integrate the hyper-dimensional gap integrals with a sufficient degree of accuracy; and may be naturally and efficiently extended to represent contact between higher-order surfaces. The efficacy of the method is demonstrated on several benchmark problems. Continuing and future work is also discussed, with a focus on intended applications and extensions of the method.

1 MODEL PROBLEM DESCRIPTION

Consider two continuum bodies $\Omega_\alpha \, \forall \alpha = 0, 1$ which lie in $\mathbb{R}^n$ that share a common interface $\Gamma = \partial\Omega_0 \cap \partial\Omega_1$ defined over a subset of the their boundaries $\Gamma = \Gamma_\alpha \subset \partial\Omega_\alpha \, \forall \alpha = 0, 1$. For the model problem under consideration, suppose these two bodies are kinematically tied along this shared interface such that

$$\mathbf{x}_1 - \mathbf{x}_0 = \mathbf{0} \quad \forall \mathbf{x}_\alpha \in \Gamma_\alpha, \; \alpha = 0, 1. \tag{1}$$

The above equality constraint may be equivalently enforced by introducing a Lagrange multiplier field $\boldsymbol{\lambda} \in \mathcal{F}(\Gamma)$ with units of surface traction (force per unit area) defined over Γ such that

$$\int_\Gamma (\mathbf{x}_1 - \mathbf{x}_0) \cdot \boldsymbol{\lambda} \, \mathrm{d}\Gamma = 0 \quad \forall \boldsymbol{\lambda} \in \mathcal{F}(\Gamma). \tag{2}$$

2 DEFINITION OF A CONTINUOUS FAMILY OF INTERMEDIATE INTERFACES

In the mathematical formulation of the model problem, there is no ambiguity regarding the particular choice of Γ since both Γ_0 and Γ_1 are coincident. However, in the numerical setting, each Γ_α may be discretized (e.g. using finite elements) in a non-conforming manner, and it is not immediately clear how Γ should be defined.

Suppose that there exists a continuous family of intermediate interfaces Γ_α parameterized by $\alpha \in [0, 1]$, as depicted in Figure 1. When $\alpha = 0$ or 1, one identifies the surfaces Γ_0 and Γ_1 that respectively lie on the boundaries of each body, i.e. $\Gamma_0 \subset \partial\Omega_0$ and $\Gamma_1 \subset \partial\Omega_1$. For all other values of $\alpha \in (0, 1)$, a range of intermediate surfaces are defined which constitute a continuous interpolation between Γ_0 and Γ_1. The continuous collection of all such intermediate surfaces spanning $\alpha \in [0, 1]$ may be interpreted as an intermediate domain $\Sigma = \{(\mathbf{x}_\alpha, \alpha) \,|\, \mathbf{x}_\alpha \in \Gamma_\alpha, \alpha \in [0, 1]\}$ spanning the void between Γ_0 and Γ_1. The parameter α may be regarded as an auxiliary spatial variable such that Σ represents a differentiable n-dimensional manifold embedded in $\mathbb{R}^{n+1}$, whose projection onto the original spatial domain spanning $\mathbf{x} \in \mathbb{R}^n$ has the interpretation as being a degenerate volume.

Evaluation of constraint integral expressions over Γ such as Equation (2) are typically effected via integration over Γ_α for a particular choice of $\alpha \in [0, 1]$, i.e.

$$\int_{\Gamma_\alpha} (\mathbf{x}_1 - \mathbf{x}_0) \cdot \boldsymbol{\lambda} \, \mathrm{d}\Gamma_\alpha = 0 \quad \forall \boldsymbol{\lambda} \in \mathcal{F}(\Gamma_\alpha). \tag{3}$$

For example, specification of an "average" intermediate surface $\Gamma_{\alpha=0.5}$ has been suggested by various authors [1, 2]. Commonly, however, either Γ_0 or Γ_1 ($\alpha = 0$ or 1) is chosen for the sake of evaluating surface integrals. Regardless of the choice of α, the specification of the particular domain of integration remains a point of ambiguity. Moreover, the need remains for establishing a mapping between pairs of points $\mathbf{x}_0 \in \Gamma_0$ and $\mathbf{x}_1 \in \Gamma_1$, which may not be uniquely defined.

Alternatively, rather than selecting a particular Γ_α over which to evaluate surface integral expressions as in Equation (3), the present work proposes the following integral-average over the

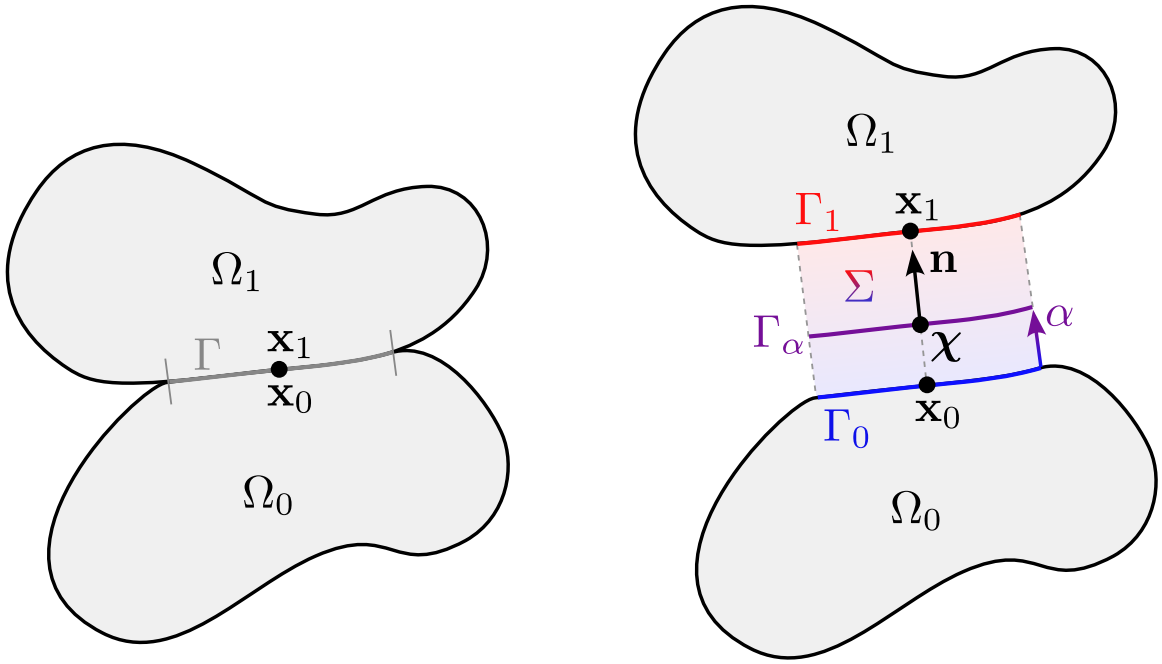

Figure 1: Conceptual illustration of a continuous collection of intermediate surfaces Γ_α parameterized by $\alpha \in [0, 1]$.

entire family of intermediate surfaces spanning $\alpha \in [0, 1]$ in the formulation and enforcement of interfacial constraints:

$$\int_{\alpha=0}^{\alpha=1} \int_{\Gamma_\alpha} \frac{\partial \mathbf{x}}{\partial \alpha} \cdot \boldsymbol{\lambda} \, \mathrm{d}\Gamma_\alpha \mathrm{d}\alpha = 0 \quad \forall \boldsymbol{\lambda} \in \mathcal{F}(\Sigma), \tag{4}$$

where the Lagrange multiplier field $\boldsymbol{\lambda}$ is presumed to be defined over the hyper-dimensional intermediate domain Σ, and $\frac{\partial \mathbf{x}}{\partial \alpha}\Delta\alpha$ represents the jump in value between $\mathbf{x}_\alpha$ and $\mathbf{x}_{\alpha+\Delta\alpha}$ in the continuous limit as $\Delta\alpha \to 0$, i.e.

$$\frac{\partial \mathbf{x}}{\partial \alpha} = \lim_{\Delta\alpha \to 0} \frac{\mathbf{x}_{\alpha+\Delta\alpha} - \mathbf{x}_\alpha}{\Delta\alpha}. \tag{5}$$

2.1 Parameterization and integration over the intermediate domain

Let the intermediate domain $\Sigma \subset \mathbb{R}^{n+1}$ be interpreted as an n-dimensional hypersurface parameterized by the set of coordinates $\boldsymbol{\xi} \in \square$ defined over a parametric domain $\square \subset \mathbb{R}^n$, from which the following parametric mapping is established: $\boldsymbol{\chi} : \square \mapsto \Sigma; \boldsymbol{\xi} \mapsto \boldsymbol{\chi}(\boldsymbol{\xi})$ and $\boldsymbol{\chi}(\boldsymbol{\xi}) = \{\mathbf{x}(\boldsymbol{\xi}), \alpha(\boldsymbol{\xi})\} \in \Sigma$. Further, let $\mathbf{J}$ denote the Jacobian of $\boldsymbol{\chi}(\boldsymbol{\xi})$:

$$\mathbf{J} = \frac{\partial \boldsymbol{\chi}}{\partial \boldsymbol{\xi}}. \tag{6}$$

For any given point $\boldsymbol{\chi} \in \Sigma$, the directed differential surface element $\mathrm{d}\boldsymbol{\Sigma} \in \mathbb{R}^{n+1}$ is determined as follows:

$$\mathrm{d}\boldsymbol{\Sigma} = \mathrm{cof}(\mathbf{J}) \cdot \mathbf{e}_\alpha \, \mathrm{d}\square, \tag{7}$$

where $\mathrm{cof}(\mathbf{J})$ denotes the matrix cofactor of $\mathbf{J}$; $\mathbf{e}_\alpha \in \mathbb{R}^{n+1}$ denotes the Cartesian basis vector aligned with the hyper-dimensional coordinate dimension associated with the parameter α (such that $\boldsymbol{\chi} \cdot \mathbf{e}_\alpha = \alpha$); and $\mathrm{d}\square$ denotes the differential form associated with the parametric domain of integration $\square$. In particular, for $n = 2$:

$$\mathrm{d}\boldsymbol{\Sigma} = \begin{vmatrix} x_{,\xi} & x_{,\eta} & \mathbf{e}_x \\ y_{,\xi} & y_{,\eta} & \mathbf{e}_y \\ \alpha_{,\xi} & \alpha_{,\eta} & \mathbf{e}_\alpha \end{vmatrix} \mathrm{d}\xi \, \mathrm{d}\eta, \tag{8}$$

and for $n = 3$:

$$\mathrm{d}\boldsymbol{\Sigma} = \begin{vmatrix} x_{,\xi} & x_{,\eta} & x_{,\zeta} & \mathbf{e}_x \\ y_{,\xi} & y_{,\eta} & y_{,\zeta} & \mathbf{e}_y \\ z_{,\xi} & z_{,\eta} & z_{,\zeta} & \mathbf{e}_z \\ \alpha_{,\xi} & \alpha_{,\eta} & \alpha_{,\zeta} & \mathbf{e}_\alpha \end{vmatrix} \mathrm{d}\xi \, \mathrm{d}\eta \, \mathrm{d}\zeta. \tag{9}$$

The projected component $\mathrm{d}\boldsymbol{\Sigma} \cdot \mathbf{e}_\alpha$ represents the differential volume of Σ measured in the original spatial domain spanning $\mathbb{R}^n$. Removal of this component from $\mathrm{d}\boldsymbol{\Sigma}$ yields:

$$\mathrm{d}\boldsymbol{\Sigma} - (\mathrm{d}\boldsymbol{\Sigma} \cdot \mathbf{e}_\alpha) \, \mathbf{e}_\alpha = \mathbf{n} \, \mathrm{d}\Gamma_\alpha \mathrm{d}\alpha, \tag{10}$$

where $\mathbf{n} \in \mathbb{R}^n$ is the unit vector that lies normal to the surface Γ_α, and $\mathrm{d}\Gamma_\alpha \mathrm{d}\alpha$ possesses the appropriate units of differential surface area (assuming α is dimensionless).

Let $\bar{\mathbf{J}}$ denote the projection of the Jacobian onto the $(n+1)$-dimensional hyperplane spanned by the differential area $\mathrm{d}\Gamma_\alpha \mathrm{d}\alpha$ with normal $\mathbf{n}$, i.e.

$$\bar{\mathbf{J}} = \mathbf{J} - (\mathbf{n} \cdot \mathbf{J}) \, \mathbf{n}. \tag{11}$$

It follows that the differential area element $\mathrm{d}\Gamma_\alpha \mathrm{d}\alpha$ is equivalently determined by

$$\mathrm{d}\Gamma_\alpha \mathrm{d}\alpha = \sqrt{\mathrm{d}\boldsymbol{\Sigma} \cdot \mathrm{d}\boldsymbol{\Sigma} - (\mathrm{d}\boldsymbol{\Sigma} \cdot \mathbf{e}_\alpha)^2} = \sqrt{\det(\bar{\mathbf{g}})} \, \mathrm{d}\square, \tag{12}$$

where $\bar{\mathbf{g}} = \bar{\mathbf{J}}^T \bar{\mathbf{J}}$ denotes the metric tensor associated with $\bar{\mathbf{J}}$. Thus, integration over the family of all intermediate surfaces may be carried out via the following integral transformation:

$$\int_{\alpha=0}^{\alpha=1} \int_{\Gamma_\alpha} (\cdot) \, \mathrm{d}\Gamma_\alpha \mathrm{d}\alpha = \int_{\square} (\cdot) \sqrt{\det(\bar{\mathbf{g}})} \, \mathrm{d}\square. \tag{13}$$

2.2 Definition of relative deformation measures

Suppose the intermediate domain undergoes a sequence of time-varying deformations, such that Σ_t denotes the deformed configuration of the intermediate domain at time t. The Jacobian consequently varies with time:

$$\mathbf{J}_t = \frac{\partial \boldsymbol{\chi}_t}{\partial \boldsymbol{\xi}}, \tag{14}$$

and $\boldsymbol{\chi}_t \in \Sigma_t$ denotes the deformed hyper-dimensional coordinates of the intermediate domain at time t. If the parameter α is interpreted as an auxiliary spatial variable, then the following relative deformation measure may be defined, akin to a deformation gradient:

$$\mathbf{F}_t = \frac{\partial \boldsymbol{\chi}_t}{\partial \bar{\boldsymbol{\chi}}_0} = \begin{bmatrix} \frac{\partial \mathbf{x}_t}{\partial \bar{\mathbf{x}}_0} & \frac{\partial \mathbf{x}_t}{\partial \alpha_0} \\ \frac{\partial \alpha_t}{\partial \bar{\mathbf{x}}_0} & \frac{\partial \alpha_t}{\partial \alpha_0} \end{bmatrix} = \mathbf{J}_t \bar{\mathbf{J}}_0^{\dagger}, \tag{15}$$

where $\bar{\mathbf{J}}_0^{\dagger}$ denotes the left pseudoinverse of $\bar{\mathbf{J}}_0$, computed as

$$\bar{\mathbf{J}}_0^{\dagger} = \bar{\mathbf{g}}_0^{-1} \bar{\mathbf{J}}_0^T, \qquad \bar{\mathbf{g}}_0 = \bar{\mathbf{J}}_0^T \bar{\mathbf{J}}_0, \tag{16}$$

and $\bar{\mathbf{J}}_0$ is defined as the projected Jacobian from Equation (11) evaluated at $t = 0$. As defined in Equation (5), the deformation quantity $\frac{\partial \mathbf{x}_t}{\partial \alpha_0} \in \mathbb{R}^n$ provides a local measure of the relative separation between Γ_α and $\Gamma_{\alpha+\Delta\alpha}$, and may consequently be evaluated as:

$$\frac{\partial \mathbf{x}_t}{\partial \alpha_0} = \frac{\partial \mathbf{x}_t}{\partial \boldsymbol{\xi}} \bar{\mathbf{g}}_0^{-1} \frac{\partial \alpha_0}{\partial \boldsymbol{\xi}}. \tag{17}$$

In all subsequent discussions, subscripts indicating the time of evaluation for the aforementioned quantities are omitted, and it is understood that the motion of the intermediate domain is measured relative to a given reference configuration, nominally Σ_0.

The component of $\frac{\partial \mathbf{x}}{\partial \alpha}$ that lies normal to Γ_α measures the locally defined normal separation (gap), whereas the component of $\frac{\partial \mathbf{x}}{\partial \alpha}$ that lies tangent to Γ_α represents the relative tangential slip between the surfaces of interest. Owing to the manner in which $\frac{\partial \mathbf{x}}{\partial \alpha}$ has been defined, $\frac{\partial \mathbf{x}}{\partial \alpha} = \mathbf{0}\ \forall \boldsymbol{\chi}$ only when the two surfaces Γ_0 and Γ_1 are coincident.

2.3 Discretization into finite elements

Suppose that both bodies Ω_0 and Ω_1 are discretized into finite elements. Additionally, suppose that the intermediate domain between Γ_0 and Γ_1 may also be discretized into a collection of hyper-dimensional "gap" finite elements $\sigma_e \subset \Sigma$. In this regard, the proposed method bears similarity to other volume-based contact discretization methods, such as the contact domain method [3, 4] and the third medium approach [5]. However, the treatment of the intermediate volume as a hyper-dimensional domain through introduction of the variable α constitutes a distinguishing novelty of the present work.

For the present discussion, low-order isoparametric finite elements (linear and quadratic triangles and quadrilaterals) are considered, although the proposed methodology may be directly generalized to the case of higher-order elements. All integrals are evaluated using standard Gaussian quadrature rules defined over each element.

Let the hyper-dimensional coordinates $\boldsymbol{\chi} \in \Sigma$ be regarded as nodally interpolated fields, represented in terms of the set of all finite element basis functions $\{\varphi_a\}_{a=1}^{N_{nodes}}$ defined over Σ:

$$\boldsymbol{\chi}(\boldsymbol{\xi}) = \sum_{a=1}^{N_{nodes}} \boldsymbol{\chi}_a \, \varphi_a(\boldsymbol{\xi}). \tag{18}$$

The relative deformation measure defined in Equation (17) is therefore evaluated as:

$$\frac{\partial \mathbf{x}}{\partial \alpha} = \sum_{a=1}^{N_{nodes}} \mathbf{x}_a \frac{\partial \varphi_a}{\partial \alpha}, \qquad \frac{\partial \varphi_a}{\partial \alpha} = \frac{\partial \varphi_a}{\partial \boldsymbol{\xi}} \bar{\mathbf{g}}^{-1} \frac{\partial \alpha}{\partial \boldsymbol{\xi}}. \tag{19}$$

In the present work, the Lagrange multiplier field $\boldsymbol{\lambda} \in \mathcal{F}(\Sigma)$ is represented using the same set of basis functions as those used to represent $\frac{\partial \mathbf{x}}{\partial \alpha}$, namely:

$$\boldsymbol{\lambda} = \sum_{a \in \mathcal{A}} \boldsymbol{\lambda}_a \frac{\partial \varphi_a}{\partial \alpha}, \tag{20}$$

where $\mathcal{A} = \{a \in 1, \ldots, N_{nodes} \,|\, \alpha_a \neq 0\}$. Notably, $\left\{ \frac{\partial \varphi_a}{\partial \alpha} \right\}_{a \in \mathcal{A}}$ constitute a linearly independent set of basis functions, and form a partition of unity over Σ, i.e.

$$\sum_{a \in \mathcal{A}} \alpha_a \frac{\partial \varphi_a}{\partial \alpha} = 1 \quad \forall \boldsymbol{\chi} \in \Sigma. \tag{21}$$

Moreover, it may be shown that the resulting constraint enforced by Equation (4) using the indicated choice for $\boldsymbol{\lambda}$ is obtained equivalently as the solution to the following $L^2(\Sigma)$ minimization problem:

$$\min_{\mathbf{x} \in \Sigma \setminus \Gamma_0} \frac{1}{2} \int_{\alpha=0}^{\alpha=1} \int_{\Gamma_\alpha} \frac{\partial \mathbf{x}}{\partial \alpha} \cdot \frac{\partial \mathbf{x}}{\partial \alpha} \, \mathrm{d}\Gamma_\alpha \mathrm{d}\alpha. \tag{22}$$

All nodes defined on Γ_0 are regarded as independent degrees of freedom, whereas all other nodes defined over Σ (including Γ_1) are kinematically constrained. The multiplier space for the ensuing constraint enforcement procedure consequently resembles that of a mortar method [1].

3 IMPLEMENTATION AND DEMONSTRATION

The proposed method was implemented in a two-dimensional setting, and verified through several common linear elastic finite element benchmark problems. The results of these investigations are summarized in the subsequent subsections.

3.1 Linear and quadratic patch tests

Two variants on the tied contact patch test in two dimensions are considered herein, each consisting of two independently discretized elastic blocks which are kinematically tied along a shared interface. In both problem variants, horizontal displacements are constrained along the left edge of the assembly, while the bottom right corner is constrained against vertical displacement. The first problem is consistent with the standard linear finite element patch test, with a uniform normal traction imposed on the right face of the assembly. The second problem is the quadratic bending patch test, with a linearly varying normal traction imposed on the right face of the assembly. Representative illustrations of both problems are depicted in Figure 2.

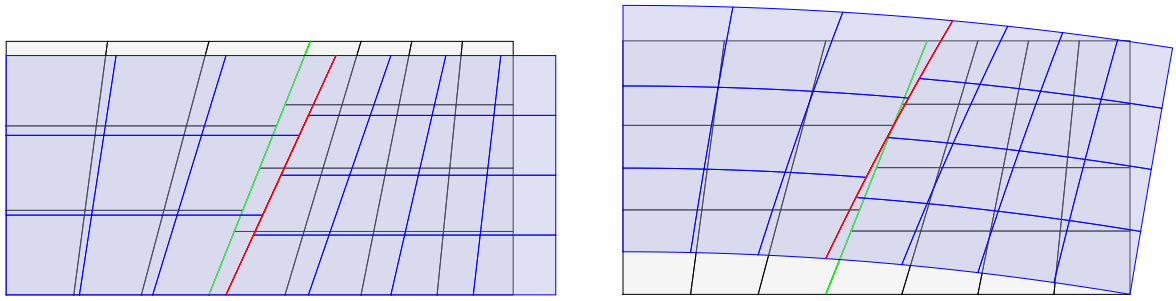

(a) (b)

Figure 2: Depictions of the patch test problem variants in two dimensions: (a) linear patch test; (b) quadratic bending patch test. The initial mesh geometry is shown in black, whereas the deformed geometry is shown in blue. The tied interface is shown in green/red in its initial/deformed configurations, respectively.

When using either linear or quadratic finite elements for the linear patch test problem, solution errors measured in the relative L^2 displacement and H^1 stress error norms were determined to be on the order of machine precision. For the quadratic patch test discretized using quadratic elements, solution errors were likewise on the order of machine precision. These results confirm that the proposed method satisfies both linear and quadratic patch tests, and is therefore capable of reproducing exact solutions with linearly and quadratically varying solution fields. Notably, sufficient solution accuracy is achieved when standard Gaussian quadrature rules are employed to evaluate constraint integrals over the discretized intermediate domain, highlighting the relative computational efficiency of the method.

3.2 Convergence Under Mesh Refinement

To investigate the convergence properties of the proposed method under mesh refinement, a simple demonstration problem was considered consisting of a long hollow cylinder with an internal pressure load. The cylinder was idealized as an equivalent two-dimensional problem under plane strain conditions, and was further simplified using the assumption of quarter symmetry. The problem geometry was decomposed into two separate hollow cylinders nested inside of one another with a tied interface defined along their shared boundary, as depicted in Figure 3. The numerical solutions obtained for this problem using both linear and quadratic discretizations were compared against the exact solution [6], with the resulting solution errors plotted in Figure 4.

Using linear elements, average convergence rates of 1.99 and 0.98 were respectively obtained in the L^2 displacement and H^1 stress error norms. Using quadratic elements, these rates were 2.96 and 1.85, respectively. The obtained results demonstrate the ability of the proposed method to achieve the desired rates of convergence under mesh refinement when a curved interface is present.

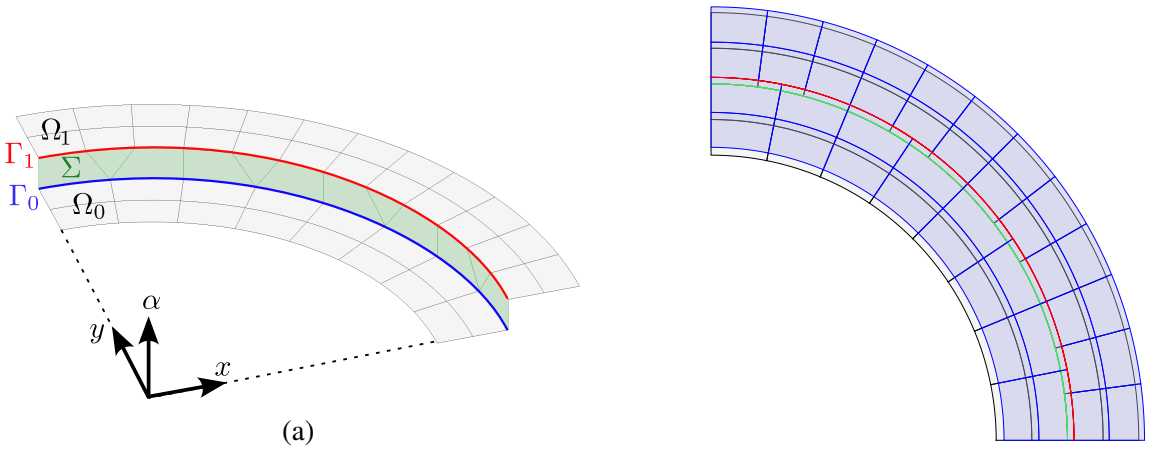

(a) (b)

Figure 3: Depictions of the pressurized hollow cylinder problem: (a) the problem geometry, including the representation of the hyper-dimensional intermediate domain Σ and its discretization into finite elements; (b) problem geometry before (black) and after deformation (blue).

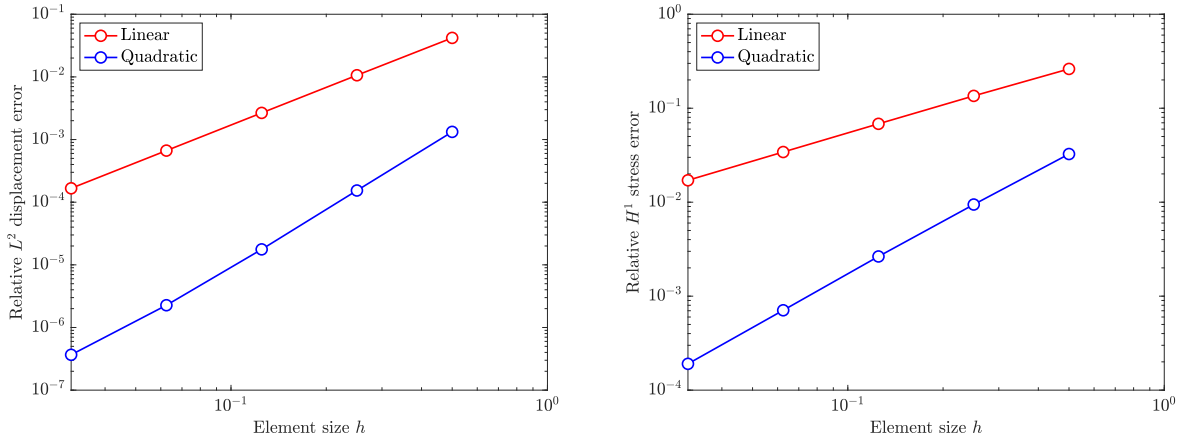

(a) (b)

Figure 4: Comparison of convergence rates under mesh refinement using linear and quadratic finite elements in the (a) relative L^2 displacement and (b) H^1 stress error norms for the pressurized cylinder problem.

4 CONCLUSIONS AND FUTURE WORK

The present explored a novel methodology for the enforcement of interfacial constraints. Within the proposed approach, the intermediate domain between two contacting interfaces is interpreted as a continuous family of intermediate surfaces parameterized by a scalar field vari-

able. If this additional field is interpreted as an auxiliary spatial coordinate, then the resulting family of surfaces may be viewed as a hyper-dimensional manifold over which constraint integrals may be formulated and evaluated. The intermediate domain may be discretized into finite elements to facilitate efficient numerical integration of constraint integrals. Initial investigations presented in this work verify that the proposed method achieves appropriate accuracy and rates of convergence for several benchmark problems. Future work will seek to extend the proposed approach to accommodate more general contact constraints with sliding and separation, with additional demonstrations for problems in three dimensions.

REFERENCES

[1] T. W. McDevitt and T. A. Laursen. A mortar-finite element formulation for frictional contact problems. *International Journal for Numerical Methods in Engineering*, 48(10):1525–1547, 2000.

[2] M.A. Puso and J.M. Solberg. A dual pass mortar approach for unbiased constraints and self-contact. *Computer Methods in Applied Mechanics and Engineering*, 367:113092, 2020.

[3] J. Oliver, S. Hartmann, J.C. Cante, R. Weyler, and J.A. Hernández. A contact domain method for large deformation frictional contact problems. part 1: Theoretical basis. *Computer Methods in Applied Mechanics and Engineering*, 198(33):2591–2606, 2009.

[4] S Hartmann, R Weyler, J Oliver, JC Cante, and JA Hernández. A 3d frictionless contact domain method for large deformation problems. *Computer Modeling in Engineering and Sciences (CMES)*, 55(3):211, 2010.

[5] P Wriggers, J Schröder, and A Schwarz. A finite element method for contact using a third medium. *Computational Mechanics*, 52:837–847, 2013.

[6] SP Timoshenko and JN Goodier. *Theory of Elasticity*. McGraw-Hill, New York, 1970.